Thermal conductivity across the phase diagram of cuprates: Low-energy quasiparticles and doping dependence of the superconducting gap

Mike Sutherland, D. G. Hawthorn, R. W. Hill, F. Ronning, S. Wakimoto, H. Zhang, C. Proust,* Etienne Boaknin, C. Lupien,[†] and Louis Taillefer[‡]

Canadian Institute for Advanced Research, Department of Physics, University of Toronto, 60 St. George Street, Toronto, Ontario, Canada M5S 1A7

Ruixing Liang, D. A. Bonn, and W. N. Hardy

Department of Physics, University of British Columbia, 6224 Agricultural Road, Vancouver, B.C., Canada V6T 1Z1

Robert Gagnon

Department of Physics, McGill University, 3600 University Street, Montréal, Québec, Canada H3A 2T8

N. E. Hussey

Department of Physics, University of Bristol, Tyndall Avenue, Bristol, BS8 1TL, United Kingdom

T. Kimura, M. Nohara, and H. Takagi

Department of Advanced Materials Science, Graduate School of Frontier Sciences, University of Tokyo, Hongo 7-3-1, Bunkyo-ku, Tokyo 113-8656, Japan

Heat transport in the cuprate superconductors $YBa_2Cu_3O_y$ and $La_{2-x}Sr_xCuO_4$ was measured at low temperatures as a function of doping. A residual linear term κ_0/T is observed throughout the superconducting region and it decreases steadily as the Mott insulator is approached from the overdoped regime. The low-energy quasiparticle gap extracted from κ_0/T is seen to scale closely with the pseudogap. The ubiquitous presence of nodes and the tracking of the pseudogap shows that the overall gap remains of the pure d-wave form throughout the phase diagram, which excludes the possibility of a complex component (ix) appearing at a putative quantum phase transition and argues against a nonsuperconducting origin to the pseudogap. A comparison with superfluid density measurements reveals that the quasiparticle effective charge is weakly dependent on doping and close to unity.

I. INTRODUCTION

In a d-wave superconductor, the presence of nodes in the gap structure imposed by symmetry leads to quasiparticle excitations down to zero energy in the presence of even small amounts of disorder.[1,2] These excitations are delocalized and carry both charge and heat. The most striking property of this residual normal fluid is its universal conduction,[3] whereby quasiparticle transport is independent of impurity concentration. In the case of heat transport, it turns out to be a direct measure of the low-energy quasiparticle spectrum.[4] The universal character of heat transport was confirmed experimentally for the cuprates $YBa_2Cu_3O_y$ (YBCO) (Ref. 5) and $Bi_2Sr_2CaCu_2O_8$ (Bi-2212).[6] Moreover, the residual heat conduction measured at optimal doping[7] or above, in the overdoped regime,[8] is in good quantitative agreement with d-wave BCS theory and the quasiparticle spectrum either measured by angle-resolved photoemission spectroscopy (ARPES) or expected from estimates based on the value of T_c (see, for instance, Ref. 7).

In this paper, we use the well-established and robust connection between low-temperature heat transport and the energy spectrum of a d-wave superconductor to probe the evolution of low-energy quasiparticles and the superconducting gap as a function of doping in the cuprates. In going from the overdoped to the underdoped regime, we find that the residual linear term κ_0/T is finite everywhere and decreases monotonically. As a result the low-energy gap grows steadily, in contrast to the superconducting T_c which first rises and then decreases. The low-energy gap in fact follows closely the normal-state pseudogap, measured mostly at higher energies and temperatures.[9] The ubiquitous presence of nodes and the tracking of the pseudogap shows that the gap remains of the pure d-wave form throughout the phase diagram. This excludes the possibility of a complex component (ix) appearing at a putative quantum phase transition and argues against a nonsuperconducting origin to the pseudogap.

II. SAMPLES

We performed our study on two cuprate materials: the double-plane orthorhombic material $YBa_2Cu_3O_y$ (YBCO) doped with oxygen in CuO chains, and the single-plane material $La_{2-x}Sr_xCuO_4$ doped with Sr atoms (LSCO). The four samples of YBCO used in the study are detwinned, flux-grown single crystals in the shape of platelets with typical dimensions 1.0×0.5 mm and 25 μm thick. Two of them, respectively with $y=6.99$ and $y=6.54$, were grown in a $BaZrO_3$ (BZO) crucible,[10] which results in crystals with very

high chemical purity (99.99 – 99.995%) and a high degree of crystalline perfection as compared with crystals grown in Y_2O_3-stabilized ZrO_2 (YSZ) crucibles. The sample with $y = 6.99$ was detwinned at $250 \, °C$ under uniaxial stress, and then annealed at $350 \, °C$ for 50 days, resulting in CuO chains with less than 0.2% oxygen vacancies, and hence very close to the stoichiometric composition at $y = 7.00$.[10] This level of oxygen doping is slightly above that for maximal T_c (93.6 K), resulting in $T_c = 89$ K. The sample with $y = 6.54$ was similarly detwinned and then annealed at $84 \, °C$ for 2 days followed by $60 \, °C$ for 5 days. This resulted in a highly ordered ortho-II arrangement of oxygen atoms in CuO chains, with alternating full and empty chains. The other two YBCO samples, respectively with $y = 6.95$ and $y = 6.6$, were grown in a YSZ crucible, and are characterized by an impurity concentration typically one order of magnitude higher. The oxygen vacancies in the CuO chains are not ordered for these crystals. The $y = 6.6$ sample was quenched into an ice water bath after annealing, resulting in a higher level of disorder among the oxygen vacancies and thus a lower T_c as compared to nonquenched samples with similar oxygen content.

The $La_{2-x}Sr_xCuO_4$ (LSCO) samples were all grown in an image furnace using the traveling-solvent floating-zone technique and have Sr dopings of $x = 0.06$ (samples A and B), 0.07, 0.09, 0.17, and 0.20. In addition, a nonsuperconducting LSCO sample with $x = 0.05$ was also measured. With the exception of $x = 0.06$ B, all samples were measured as grown. This may result in off-stoichiometric oxygen content in the samples. The $x = 0.06$ B sample was annealed in flowing argon overnight at $800 \, °C$ in an attempt to fix the oxygen content. The argon annealing, however, had little effect on our results as both $x = 0.06$ samples gave the same electronic contribution to the thermal conductivity.

In LSCO, the hole concentration per Cu in the CuO_2 planes p is taken to be the Sr concentration x. In YBCO, however, the relation between hole concentration and oxygen doping y is a complicated function. As a result, for YBCO p is determined from transition temperatures using the empirical formula[11]

$$\frac{T_c}{T_c^{max}} = 1 - 82.6(p - 0.16)^2, \tag{1}$$

which is a good approximation for many cuprate systems.[12] Here we use $T_c^{max} = 93.6$ K as the transition temperature of optimally doped YBCO.

The transition temperature was determined from resistivity measurements and defined as the temperature at which the resistivity has fallen to 1% of the value prior to the onset of the superconducting transition. Note that this definition of T_c leads to values slightly lower than those determined by taking the midpoint of the resistive transition. We find, however, that values of T_c determined this way correlate well with those measured by magnetic susceptibility and thermal conductivity. For the YBCO samples, the transition temperatures are 62, 44, 93.5, and 89 K, respectively, for oxygen doping $y = 6.54$, 6.6, 6.95, and 6.99. We note that the T_c for the ortho-II ordered $y = 6.54$ appears anomalously high. This

enhanced T_c (consistent with the T_c determined by magnetization measurements in similar samples[13]) is thought to be due to oxygen coordination effects, where improved oxygen ordering leads to a greater number of holes doped into the CuO_2 planes as compared to a nonordered crystal with the same nominal oxygen doping.[14] For the LSCO samples, the transition temperatures are 5.5, 8.5, 19, 16, 34, and 33.5 K, respectively, for Sr doping $x = 0.06$ (sample A, not annealed), 0.06 (sample B, annealed), 0.07, 0.09, 0.17, and 0.20. The T_c for the $x = 0.09$ sample is anomalously low, possibly as a result of Sr inhomogeneity or oxygen nonstoichiometry within the crystal. Although different criteria may be used for determining the value of hole doping level in both the LSCO and YBCO systems, we note that small errors in our estimation of hole concentration do not noticeably affect the trends observed in our thermal conductivity data.

The low-temperature thermal conductivity measurements were made in a dilution refrigerator down to 40 mK, using the standard four-wire steady-state method with two RuO_2 chip thermometers, calibrated *in situ* against a reference Ge thermometer. Currents were applied along the a axis in order to probe in-plane transport and to avoid contributions from the CuO chains in YBCO. Thermal and electrical contact to the samples was made using Ag wire and diffused Epotek H20E Ag-epoxy pads.

III. LEVELS OF DISORDER

It is instructive to estimate the relative amounts of disorder in our samples. For the YBCO samples, the inclusion of impurities during growth is greatly reduced by using BZO over YSZ crucibles. Microwave spectroscopy measurements of thermally excited quasiparticles in the elastic scattering limit reveal that the scattering rate in the superconducting state is some 12 times greater for optimally doped YBCO grown in YSZ crucibles[15] compared to the slightly overdoped $y = 6.99$ samples grown in BZO crucibles.[16] Measurements of thermal conductivity κ at high temperature, shown in Fig. 1, lead to a similar order-of-magnitude difference. In the theory of Hirschfeld and Putikka,[17] the peak observed in the thermal conductivity is due to an increase in the quasiparticle mean free path when the sample is cooled below T_c. The magnitude of κ continues to increase with cooling until it becomes limited by quasiparticle scattering from impurities and dislocations. Thus the ratio of peak height to normal-state value in $\kappa(T)$ directly reflects the amount of disorder present in the crystal.

The inset in Fig. 1 shows theoretical curves that demonstrate this effect,[17] where the electronic contribution to thermal conductivity normalized by the value of κ at T_c is plotted as a function of T/T_c. A large ratio of impurity scattering rate (given by Γ) to T_{c0} in these curves is seen to lead to a peak height that is suppressed. Here Γ represents the rate at which quasiparticles are scattered elastically within the sample. An order of magnitude increase in the intrinsic level of disorder within the crystal results roughly in a factor of 2 decrease in the peak height. The data presented for our crystals in Fig. 1 reflects that effect. The deliberate addition of impurities such as Zn in YSZ-grown optimally doped YBCO
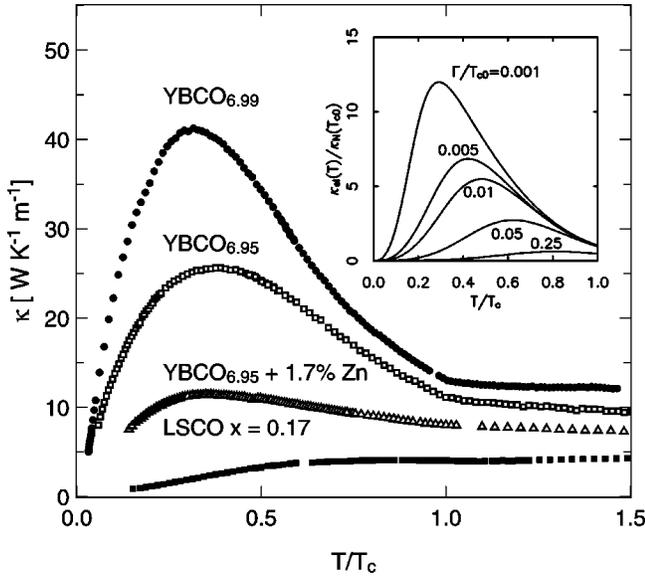
FIG. 1. Thermal conductivity of $YBa_2Cu_3O_y$ and $La_{2-x}Sr_xCuO_4$ vs temperature normalized at T_c. Inset: theoretical calculation of the effect of impurity scattering on the electronic thermal conductivity of cuprates (from Ref. 17).

FIG. 2. Thermal conductivity of $YBa_2Cu_3O_y$ plotted as κ/T vs T^2. Open symbols represent samples grown in YSZ crucibles and filled symbols those grown in BZO crucibles.

samples leads to a large suppression in peak height. Data for a sample with 1.7% Zn impurities (determined from T_c suppression) are shown in Fig. 1, and it is seen that the addition of this level of impurities causes the peak to nearly vanish. The corresponding residual resistivity extrapolated from the linear temperature dependence of $\rho_a(T)$ goes from being negative in the nominally pure crystal to $\rho_0=30$ $\mu\Omega$ cm in the Zn-doped crystal. It is clear that the optimally doped LSCO sample ($x=0.17$) shown in Fig. 1, with $\rho_0 = 33$ $\mu\Omega$ cm (as extrapolated from resistivity data above T_c), exhibits much stronger scattering than any of the YBCO samples. This is true despite the high chemical purity of the crystal, and is likely a result of the Sr atoms included as dopants acting also as scatterers. Considering all the evidence from microwave, resistivity, and heat transport measurements we estimate the relative amount of disorder in the various crystals studied here to be roughly in the proportion of 100:10:1 for LSCO, YSZ-grown YBCO, and BZO-grown YBCO, respectively.

IV. DOPING DEPENDENCE OF κ_o/T

The low-temperature thermal conductivity of YBCO and LSCO samples is shown as a function of temperature in Figs. 2 and 3, respectively. The data are plotted as κ/T vs T^2 because the quantity of interest is the residual linear term κ_o/T, defined as the $T=0$ limit of κ/T, obtained by extrapolation of the low-temperature data. This residual linear term can only be due to fermionic carriers and is attributed to zero-energy quasiparticles. Indeed, as will be seen below, it is a direct confirmation, via a robust bulk measurement, of the d-wave nature of the superconducting order parameter in cuprates. The extrapolation procedure is described in detail in the Appendix, where the contribution of phonons is analyzed. The main results of the paper do not depend on the
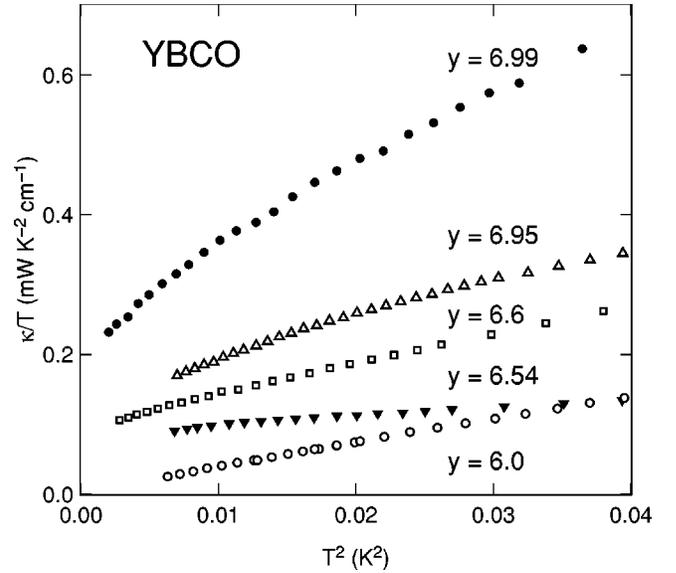
particular extrapolation procedure. This is true, for example, for the overall trend with doping, which is immediately evident from Figs. 2 and 3: κ_o/T decreases steadily with underdoping, all the way from the slightly overdoped to the highly underdoped regime. Using the extrapolation procedure outlined in the Appendix, the values we obtain are given in Table I. Note that a measurement on a fully deoxygenated YBCO sample with $y=6.0$ correctly yields a zero intercept: $\kappa_o/T=0\pm1$ μW K^{-2} cm^{-1}. The values for LSCO agree with those published in a previous study,[18] with the exception of their $x=0.17$ sample which has been measured to be approximately twice the value we observe. We attribute this difference to the fact that the crystal studied by Takeya *et al.* had a T_c of 40.2 K compared to our T_c of 34.2 K, pointing to a slightly higher hole concentration (likely due to different oxygen levels within the crystals).

Let us analyze these results within the framework of standard d-wave BCS theory. For a clean d-wave superconductor with a random distribution of impurities, an energy scale γ develops below which the density of states is approximitely constant and nonzero.[19] The magnitude of γ, known as the impurity bandwidth, is related to both the concentration of impurities, and their scattering strength. In the clean limit, when $k_BT\ll\gamma\ll k_BT_c$, the quasiparticle thermal conductivity can be written as[4]

$$\frac{\kappa_0}{T} = \frac{k_B^2}{3\hbar}\frac{n}{d}\left(\frac{v_F}{v_2} + \frac{v_2}{v_F}\right), \tag{2}$$

where n is the number of CuO_2 planes per unit cell and d is the c-axis lattice constant. Here γ, the width (in energy) of the region of constant density of states created by the presence of impurities, should not be confused with Γ, the scattering rate due to the presence of such impurities. v_F and v_2 are the quasiparticle velocities normal and tangential to the Fermi surface at the node, respectively, and are the only two
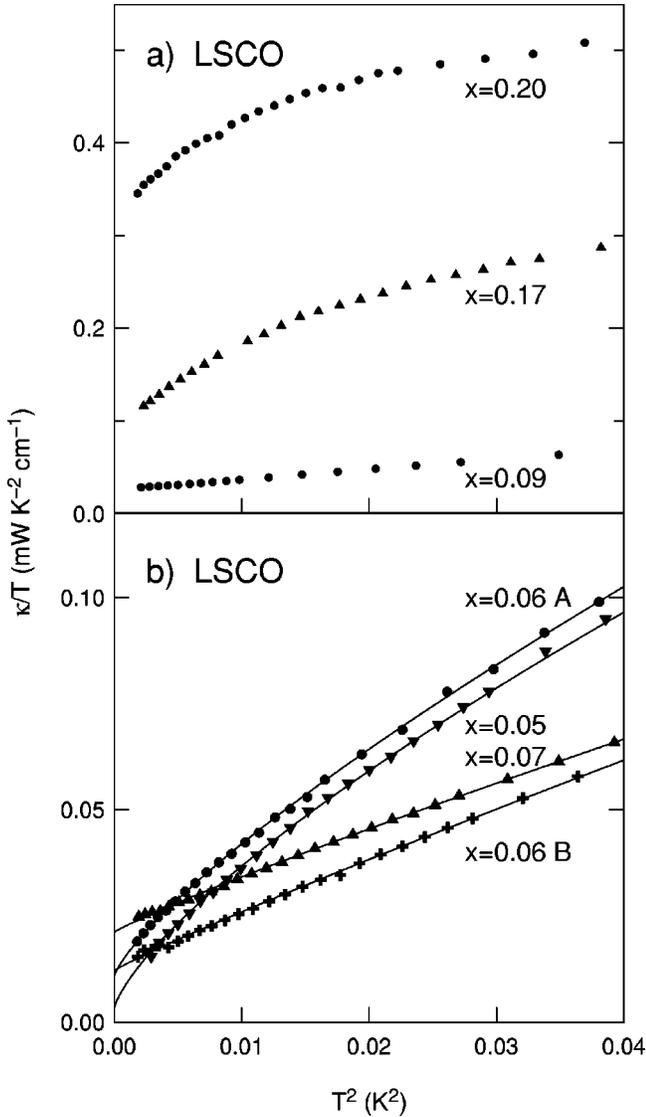
FIG. 3. Thermal conductivity of $La_{2-x}Sr_xCuO_4$ plotted as κ/T vs T^2, for (a) $x=0.09$, 0.17, and 0.20, and (b) $x=0.05$, 0.06, and 0.07. The lines through the data are power-law fits, discussed in the Appendix.

parameters that enter the low-energy spectrum, given by $E = \hbar\sqrt{v_F^2 k_1^2 + v_2^2 k_2^2}$ where $\hat{\mathbf{k}}_1$ and $\hat{\mathbf{k}}_2$ are vectors normal and tangential to the Fermi surface at the node, respectively. The parameter v_2 is simply the slope of the gap at the node:

$$\mathbf{v_2} = \frac{1}{\hbar}\frac{d\Delta}{d\mathbf{k}}\bigg|_{node} = \frac{1}{\hbar k_F}\frac{d\Delta}{d\phi}\bigg|_{node} = v_2\hat{\mathbf{k}}_2, \qquad (3)$$

where k_F is the Fermi wave vector at the nodal position. These are remarkably simple formulas, which provide a direct access to the parameters that govern low-energy phenomena in a d-wave superconductor. The residual heat conduction in Eq. (2) is not only universal, i.e., independent of scattering rate (or impurity bandwidth), but it was also shown to be independent of Fermi-liquid corrections and vertex corrections (i.e., corrections due to anisotropic scattering

TABLE I. Compilation of T_c, doping and residual linear term in the thermal conductivity, as well as values of the quasiparticle anisotropy ratio v_F/v_2 from Eq. (2) and gap maximum Δ_0 (see caption of Fig. 6) for the samples in this study. Data for optimally doped Bi-2212 (Ref. 7) and overdoped Tl-2201 (Ref. 8) from previous studies are provided for completeness.

Sample	T_c [K]	p $\left[\frac{\mu W}{K^2\,cm}\right]$	κ_0/T	v_F/v_2 [meV]	Δ_0
$YBCO_{6.0}$		0.0	0 ± 1		
$YBCO_{6.54}$	62	0.10	85 ± 10	7.9	71
$YBCO_{6.6}$	44	0.08	91 ± 13	8.7	66
$YBCO_{6.95}$	93.5	0.16	120 ± 12	11.5	50
$YBCO_{6.99}$	89	0.18	160 ± 12	15.5	37
LSCO 0.05		0.05	3 ± 1		
LSCO 0.06 A	5.5	0.06	11 ± 2		
LSCO 0.06 B	8.5	0.06	12 ± 2		
LSCO 0.07	19	0.07	22 ± 2	1.9	
LSCO 0.09	16	0.09	26 ± 10	2.4	
LSCO 0.17	34	0.17	96 ± 7	10.4	
LSCO 0.20	33.5	0.20	330 ± 40	36	
Bi-2212	89	0.16	150 ± 30	19	30
Tl-2201	15	0.26	1400 ± 70	270	2

between nodes).[4] Note, however, that the latter two corrections affect the microwave (charge) conductivity (see below).

In Fig. 4, the anisotropy ratio v_F/v_2 is plotted against carrier concentration p, using Eq. (2) and the values of κ_0/T listed in Table I. Also included is the published value for
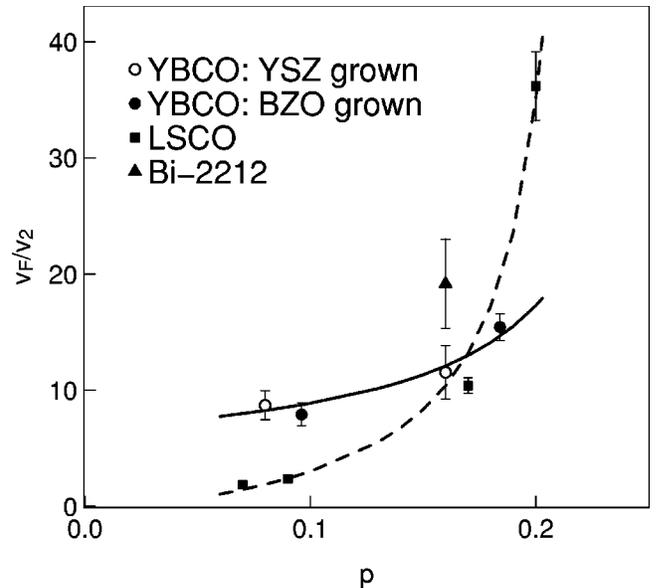
FIG. 4. Anisotropy ratio v_F/v_2, calculated from thermal conductivity data via Eq. (2), vs hole doping per CuO_2 plane p. The data for Bi-2212 are from Ref. 7. Lines are guides to the eye (solid for YBCO, dashed for LSCO).

Bi-2212 at optimal doping.[7] All three cuprates have a comparable anisotropy ratio at optimal doping: $v_F/v_2 = 10$, 12, and 19, for LSCO, YBCO, and Bi-2212, respectively. It has already been noted[7] that the value of 19 for Bi-2212 is in excellent agreement with the ratio of 20 coming from values of $v_F = 2.5 \times 10^7$ cm/s and $v_2 = 1.25 \times 10^6$ cm/s obtained directly from ARPES.[20] (Note that the value of 12 for the optimally doped YBCO crystal differs slightly—albeit within error bars—from our previously published result of 14, which was an average of several samples.[7])

V. DISCUSSION

A. Nature of the superconducting order parameter

Several authors have proposed the existence of a quantum critical point within the superconducting dome in the phase diagram of cuprates, either as a theoretical prediction to explain the diagram itself or as suggested in various experiments. Its location is usually taken to be near (or slightly above) optimal doping, in the neighborhood of $p = 0.2$. If it is associated with a change in the symmetry of the superconducting order parameter, Vojta *et al.* have argued that the most likely scenario is a transition from a pure $d_{x^2-y^2}$ state to a complex order parameter of the form $d_{x^2-y^2} + ix$, where x can have either s or d_{xy} symmetry.[21] Sharoni *et al.* have recently reported a split zero-bias anomaly in their tunneling on Y-123 thin films as soon as the material is doped beyond optimal doping, a feature which they attribute to the appearance of a complex component to the order parameter in the bulk.[22] The presence of a subdominant component ix in the order parameter causes the nodes to be removed, as the gap can no longer go to zero in any direction. Our observation of a residual linear term in the thermal conductivity of both YBCO and LSCO, as well as previous results on optimally doped Bi-2212 (Ref. 7) and strongly overdoped Tl-2201,[8] is a direct consequence of nodes in the gap. It therefore excludes the possibility of any such subdominant order parameter in the bulk throughout the doping phase diagram. In other words, if there truly is a quantum critical point inside the superconducting dome, it does not appear to be associated with the onset of a complex component in the order parameter.

In view of the ubiquitous nature of the residual linear term in superconducting cuprates, observed in four different hole-doped materials from strongly overdoped Tl-2201 to strongly underdoped LSCO, two previous results stand out as puzzling anomalies: the absence of a detectable linear term in electron-doped $Pr_{2-x}Ce_xCuO_4$ (PCCO),[23] and in hole-doped $YBa_2Cu_4O_8$.[24] In particular, note that the upper bound of 0.02 mW K^{-2} cm^{-1} quoted for κ_0/T in $YBa_2Cu_4O_8$ is four to five times lower than the value obtained here for $YBa_2Cu_3O_y$ at a comparable hole concentration ($y = 6.54$ or 6.6)—as assessed by the very similar resistivity curves above T_c—and comparable sample quality. This extremely low value is akin to that found in nonsuperconducting strongly underdoped LSCO ($x = 0.05$).
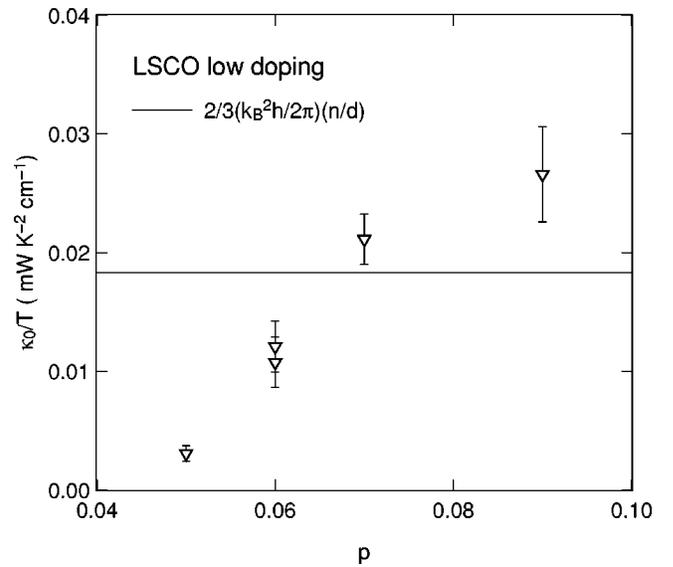
FIG. 5. Measured value of κ_0/T for highly underdoped LSCO. The solid line represents the minimum possible value allowed by Eq. (2), namely when $v_F/v_2 = 1$.

B. Effects of disorder

One of the most remarkable results of transport theory in d-wave superconductors is the universal nature of heat conduction, which appears due to a cancellation between the increase in normal-fluid density and the decrease in mean free path observed as the concentration of impurities is increased.[4] This universal behavior is only found in the clean limit where $\hbar\Gamma \ll \Delta_0$. In situations where Γ is large (or Δ_0 is small), the behavior is no longer universal, and the measured linear term may be closer to the normal-state value κ_N/T than the universal limit. In the extreme case where $\hbar\Gamma \sim \Delta_0$, superconductivity is destroyed and the normal-state value of κ_N/T is recovered. Therefore the validity of using Eq. (2) to extract values of v_F/v_2 from measurements of the residual linear term is ensured only when samples are in the clean (universal) limit, $\hbar\Gamma \ll \Delta_0$. Universal behavior in YBCO at optimal doping is already well established,[5] and inspection of Fig. 4 shows that this is confirmed at other dopings. Indeed, we observe that both BZO and YSZ grown crystals yield values of v_F/v_2 that lie on the same curve despite having an order of magnitude difference in purity level, which is strong evidence that the clean limit is reached in our YBCO samples.

In LSCO, the extremely small values of κ_0/T measured in highly underdoped samples point to a different conclusion. Indeed, for $x = 0.06$, $\kappa_0/T \simeq 12$ μW K^{-2} cm^{-1}, while the minimum value for LSCO allowed by Eq. (2) is $(k_B^2/3\hbar)(n/d)(1+1) = 18.3$ μW K^{-2} cm^{-1}. The data for the LSCO samples with the lowest dopings are plotted in Fig. 5, which shows that the use of Eq. (2) for these samples is invalid. This breakdown suggests that our underdoped LSCO samples are not in the clean limit, and hence we cannot extract quantitative information by using Eq. (2), as we will do for YBCO in the following sections. The same conclusion would apply to previous LSCO data.[18]

In order to understand the LSCO data within a *d*-wave BCS theory of low-temperature heat transport, it will be necessary to incorporate the effects of impurity scattering in the underdoped regime outside of the clean (universal) limit. The effect of impurity scattering on a *d*-wave superconductor has been worked out in the standard case of a normal state that is *metallic*, and conducts heat *better* than the superconducting state.[25] When the concentration of impurities is increased in such a case, T_c is gradually suppressed to zero and the residual linear term *rises* monotonically to meet its normal state value. However, our LSCO samples with $x \lesssim 0.09$ exhibit the well-known insulating upturns in the normal-state resistivity associated with the ground-state metal-insulator transition observed near $x \sim 0.16$.[26] In fact the resistivity in a strong magnetic field appears to diverge as $T \rightarrow 0$.[27] Thus, for the LSCO samples where $x < 0.16$, the effect of increasing the impurity concentration would be to evolve the system towards an *insulating* state, or at least one that conducts heat *less well*. In this scenario, we expect the measured residual linear term κ_0/T to be *smaller* than the universal value, which would explain how in Fig. 5 we measure a linear term smaller than that allowed by Eq. (2).

Another possibility is suggested by the theoretical work of Atkinson and Hirschfeld,[28] in which the Bogoliubov–de Gennes equations are used to model the paired state as an inhomogenous superfluid. This approach allows for the possibility of quantum interference processes such as localization which are neglected in the usual framework. In their model, the residual linear term κ_0/T is seen to decrease in the presence of increasing impurity concentration, a direct result of weak localization of carriers. The fact that we measure a linear term in underdoped LSCO which is smaller than that allowed by Eq. (2) may be evidence for the existence of such localization in LSCO. We hope these observations will stimulate further theoretical work.

C. Doping dependence of the superconducting gap

The remarkable success of Eq. (2) at optimal doping validates the extension of our study across the doping phase diagram, at least for our YBCO samples, where the clean (universal) limit is established. In interpreting our measurements of the anisotropy ratio v_F/v_2 in such a study, the first thing to emphasize is the fact that v_F, the Fermi velocity at the node, is essentially independent of doping. This was shown by ARPES both in Bi-2212 (Ref. 20) and in LSCO,[33] where the slope of the E vs k dispersion at the Fermi energy is seen to vary by no more than 10% over the range $0.03 < x < 0.3$, with an average value of $v_F \simeq 2.5 \times 10^7$ cm/s in both materials. The position of the node in k space is also independent of doping,[20] with $k_F \simeq 0.7$ Å^{-1} as measured from (π,π) to the Fermi surface. As a result, a study of κ_0/T vs p yields the doping dependence of $v_2 = v_2(p)$. In Fig. 6, we plot the slope of the gap at the node as a function of carrier concentration, not as v_2 vs p but in a more familiar guise as the corresponding gap maximum, Δ_0, of a putative *d*-wave gap function $\Delta = \Delta_0 \cos 2\phi$, via Eqs. (2) and (3). Given that k_F is constant, this is equivalent to plotting v_2 directly. The values of Δ_0 are also listed in Table I. Again,
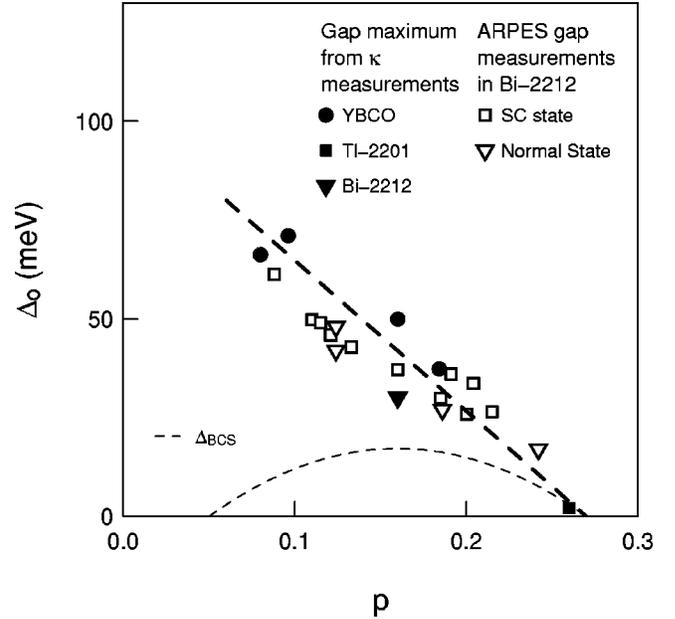
FIG. 6. Doping dependence of the superconducting gap Δ_0 obtained from the quasiparticle velocity v_2 defined in Eq. (3) (filled symbols). Here we assume $\Delta = \Delta_0 \cos 2\phi$, so that $\Delta_0 = \hbar k_F v_2/2$, and we plot data for YBCO alongside Bi-2212 (Ref. 7) and Tl-2201 (Ref. 8). For comparison, a BCS gap of the form $\Delta_{BCS} = 2.14 k_B T_c$ is also plotted, with T_c taken from Eq. (1) (and $T_c^{max} = 90$ K). The value of the energy gap in Bi-2212, as determined by ARPES, is shown as measured in the superconducting state[29] and the normal state[30–32] (open symbols). The thick dashed line is a guide to the eye.

here we have confined our analysis to YBCO only, given that LSCO was seen to lie outside the clean limit. Plotted alongside these data is a conventional BCS *d*-wave gap (dashed curve), where we have assumed $\Delta_0 = 2.14 k_B T_c$ (weak-coupling approximation). The p dependence of the gap is estimated using Eq. (1), with a maximum T_c at optimal doping of 90 K.

Let us examine the implications of these results by starting on the overdoped side of the phase diagram. The only available data in the strongly overdoped regime is on Tl-2201,[8] a single-plane cuprate with optimal $T_c \simeq 90$ K. For an overdoped crystal with $T_c = 15$ K, the measured residual linear term is $\kappa_0/T = 1.4$ mW K^{-2} cm^{-1}, which yields $v_F/v_2 = 270$ via Eq. (2). In comparison, the weak-coupling BCS prediction based on the value of $T_c = 15$ K is $v_F/v_2 = 210$, using the values of v_F and k_F given above. The good quantitative agreement shows that in this strongly overdoped regime BCS theory works quite well, and the much larger anisotropy ratio is a consequence of the much smaller T_c.

We now turn our attention to the underdoped region of the phase diagram. In the case of YBCO the decrease in κ_0/T by a factor 2 between $y = 6.99$ and $y = 6.54$ provides one of the main results of this paper: the velocity ratio decreases with underdoping; it drops from 16 to 8 in going from a sample with $T_c = 89$ K to an underdoped sample with $T_c = 62$ K. *This reflects an underlying steepening of the gap at the node while T_c drops, with underdoping.* Note that this is in con-

tradiction with the results of Mesot *et al.* who extracted a slope of the gap from their ARPES measurements on Bi-2212 near optimal doping that seemed to decrease slightly with underdoping.[20] This trend seems also to be at odds with low-temperature penetration depth measurements of Panagopoulos *et al.* who extract a Δ_0 that is strongly ϕ dependent and whose value scales with T_c in the underdoped regime when measured at the node.[34]

Taken by itself, this could be attributed either to a gradual departure from weak-coupling towards strong-coupling BCS superconductivity, with a growing ratio Δ_0/T_c. It could also be interpreted as a gradual deformation of the gap shape, from a simple $\cos 2\phi$ angular dependence to a much steeper function with a decreasing average gap that scales with T_c. However, in view of the known behavior of the pseudogap, these explanations are unlikely to be the main story. Indeed, the growth of the low-energy gap observed through κ_0/T is highly reminiscent of the similar trend observed in the pseudogap with underdoping. In fact the growth of Δ_0 derived from v_2 is in quantitative agreement with the normal-state gap maximum determined by ARPES (the pseudogap),[30-32] and the gap maximum measured at 15 K (the superconducting gap)[29] as shown in Fig. 6. In making a quantitative comparison between our data and the value of Δ_0 measured in the superconducting state by ARPES, we note that the peak position at $(\pi,0)$ is roughly equal to the gap value extracted by fitting the photoemission spectra along the Fermi surface.[35]

This striking similarity in scaling points to a common origin, which allows us to say the following things on the nature of the pseudogap. First, due to the very existence of a residual linear term, the (total) gap seen in thermal conductivity at $T \to 0$ is one that must have nodes. Second, it has a linear dispersion as in a d-wave gap (i.e., it has a Dirac-like spectrum). Third, it is a quasiparticle gap and not just a spin gap. A fundamental question is whether the pseudogap is related to or independent of superconductivity. The first and most natural possibility is that it is due to some form of precursor pairing. A second possibility is that it may come from a distinct nonsuperconducting state. Indeed, a universal thermal conductivity is also possible in a nonsuperconducting state as long as the energy spectrum is Dirac like (i.e., linear dispersion). For example, a universal (charge) conductivity was derived for a degenerate semiconductor in two-dimensions.[36] Interestingly, the d-density-wave (DDW) state proposed as an explanation for the pseudogap phenomena seen in underdoped cuprates[37] also exhibits a universal conductivity provided that the chemical potential $\mu=0$. In the region where both orders coexist—DDW and d-wave superconductivity (DSC)—Eq. (2) is then predicted to hold,[38] with v_2 replaced by $\sqrt{(v_\Delta^{DDW})^2+(v_\Delta^{SC})^2}$, where v_Δ^{DDW} and v_Δ^{SC} are the gap velocities for the two types of order, respectively. The main question then is how does the chemical potential evolve as a function of doping?

In summary, our measurements of κ/T throughout the phase diagram allow us to make the following statements about the evolution of Δ_0 with doping. First, the extrapolated value of the gap maximum from thermal conductivity in the

overdoped regime is in excellent quantitative agreement with that expected from BCS theory. Second, Δ_0 continues to grow with underdoping while T_c rises and then falls, in contradiction to what one would expect from BCS theory. The divergence of these two energy scales in the underdoped regime is a manifestation of the pseudogap, whose presence is now revealed at very low energies in a bulk measurement on crystals of the utmost quality and purity. The fact that the gap preserves its pure d-wave form (with nodes on the Fermi surface) throughout strongly suggests that the pseudogap is superconducting in origin.

D. Superfluid density and microwave conductivity

One way to shed further light on the nature of the low-energy electron state in underdoped YBCO is to compare heat transport and charge dynamics. For a d-wave BCS superconductor, Durst and Lee have shown that the two conductivities are affected differently by scattering anisotropy and quasiparticle interactions.[4] The charge conductivity in the $\omega \to 0$ and $T \to 0$ limit is given by

$$\lim_{T \to 0} \sigma_1(T) = \sigma_0 = \frac{e^2}{\hbar} \frac{1}{\pi^2} \frac{n}{d} \beta_{VC} \alpha_{FL}^2 \frac{v_F}{v_2}, \quad (4)$$

where e is the electron charge. The factor β_{VC} is due to vertex corrections and is greater than 1.0 when impurity scattering is anisotropic. This simply reflects the fact that intra-node scattering will degrade a charge current less than inter-node (opposite- or side-node) scattering that involves a larger change in momentum. This is the discrete version of the $(1 - \cos\theta)$ term that enters normal-state conductivity and reflects the predominance of backscattering over small-angle scattering. Numerical calculations suggest that β_{VC} can be large (e.g., in excess of 10) in high-purity samples as long as impurity scattering is in the unitary limit.[4] Note that vertex corrections have a negligible effect on heat transport. The factor α_{FL}^2 is a Fermi-liquid (FL) correction which arises because of quasiparticle-quasiparticle interactions. The same factor also enters in the low-temperature slope of the normal-fluid density $\rho_n(T) = \rho_s(T=0) - \rho_s(T)$:[4]

$$\frac{\rho_n(T)}{m} = \frac{2\ln2}{\pi} \frac{1}{\hbar^2} \frac{n}{d} \alpha_{FL}^2 \frac{v_F}{v_2} k_B T. \quad (5)$$

The temperature dependence of the a-axis superfluid density of YBCO crystals very similar to ours was measured via the penetration depth.[16,39] The value of $\alpha_{FL}^2(v_F/v_2)$ obtained from these data is shown in Fig. 7. Using the value of v_F/v_2 from κ_0/T (averaging the YSZ-grown and BZO-grown data) yields

$$\alpha_{FL}^2 \simeq 0.4–0.5, \quad \text{at} \quad p \simeq 0.16, \quad (6)$$

$$\alpha_{FL}^2 \simeq 0.6–0.7, \quad \text{at} \quad p \simeq 0.09. \quad (7)$$

A similar value was previously derived for optimally doped Bi-2212.[7] We conclude that this FL parameter is near unity and, more importantly, is only weakly dependent on doping. In a recent paper, Ioffe and Millis[40] argue that a
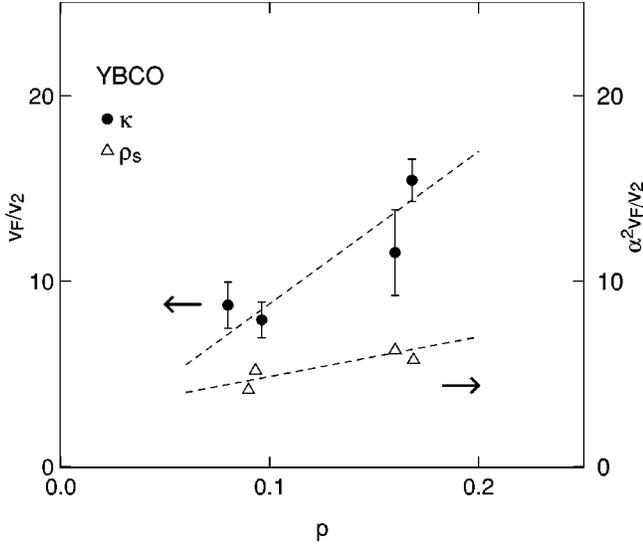
FIG. 7. Quasiparticle velocity ratio in YBCO obtained from universal heat transport, as v_F/v_2 (circles) via Eq. (2), and from superfluid density data of Refs. 16 and 42, as $\alpha_{FL}^2(v_F/v_2)$ (triangles) via Eq. (5). Lines are guides to the eye.

doping independent α_{FL}^2, interpreted as effective charge, is inconsistent with both the Brinkman-Rice mean-field theory and slave boson gauge theory approaches to the Mott physics of high-T_c materials. Indeed the combination of a doping independent α_{FL}^2 and v_F, along with a v_2 that increases with decreasing doping provides a significant challenge to microscopic theories of d-wave superconductivity in cuprates.

The microwave conductivity $\sigma_1(\omega,T)$ of YBCO was recently measured in crystals nominally identical to ours with $y=6.50$ (Ref. 39) and $y=6.99$.[16] Even though the measurements go down to 1 GHz and 1.3 K, it turns out to be unclear how to reliably extrapolate these data to the $\omega=0$ and $T=0$ limit, so that a meaningful comparison of κ_0/T and σ_0 is not quite possible at this stage. The shape and temperature dependence of the microwave spectrum for the $y=6.50$ sample for example is suggestive of nonunitary scattering close to the Born limit, implying that the low-temperature universal limit regime may not be reached by 1.3 K. Further work is needed to ascertain whether this is indeed the correct scenario.

VI. CONCLUSIONS

We have studied the evolution of thermal transport as $T \to 0$ in the cuprate superconductors YBCO and LSCO over a wide range of the doping phase diagram. The residual linear term κ_0/T is observed to be finite throughout the superconducting region. This proves that the gap always has nodes on the Fermi surface, a fact that has two implications: (i) it rules out the possibility of a multicomponent order parameter of the type $d+ix$ in the bulk, appearing at a putative quantum phase transition, and (ii) it argues strongly in favor of a superconducting origin to the pseudogap (e.g., precursor pairing). As the Mott insulator is approached, κ_0/T is observed to decrease, leading to a decreasing value of the quasiparticle

velocity anisotropy ratio v_F/v_2. This result offers some insight into the doping dependence of several important quasiparticle parameters. First, the slope of the d-wave superconducting gap at the nodes, v_2, is seen to increase steadily as doping is decreased, consistent with a growth of the gap in the underdoped regime. This is in contradiction to what one naively expects from BCS theory, where the gap scales with T_c. The gap we extract at very low energies follows closely the pseudogap measured mostly at much higher energies by other techniques. This close tracking of the pseudogap shows that the gap remains roughly of the pure d-wave form throughout the phase diagram. Second, a comparison with superfluid density reveals that the quasiparticle effective charge is weakly dependent on doping and close to unity.

The considerable difference between the magnitude of the change in κ_0/T with underdoping for the LSCO and YBCO samples provides clues as to the role of disorder in the underdoped regime. In particular, the small value of the residual linear term of the most highly underdoped LSCO samples is incompatible with the standard theory of transport for d-wave superconductors, motivating theoretical work which would incorporate the effects of impurities in a superconductor whose normal state is insulating rather than metallic in nature.

APPENDIX: PHONON THERMAL CONDUCTIVITY IN D-WAVE SUPERCONDUCTORS

In order to use thermal conductivity as a direct probe of low-energy quasiparticles in d-wave superconductors, the contribution from phonons must be reliably extracted. This may be achieved by performing experiments in the regime $T \to 0$, where the phonon mean free path becomes limited only by the physical dimensions of the sample. From simple kinetic theory, the conductivity of phonons in this boundary-limited scattering regime is given by

$$\kappa_{ph} = \frac{1}{3}\beta\langle v_{ph}\rangle\Lambda_0 T^3, \tag{A1}$$

where β is the coefficient of phonon specific heat, Λ_0 is the temperature-independent mean free path, and $\langle v_{ph}\rangle$ is a suitable average of the acoustic sound velocities. The electronic linear term is then naturally extracted by plotting thermal conductivity data as κ/T vs T^2 and interpreting the intercept as the residual linear term at $T=0$, and the slope as the phonon contribution governed by Eq. (8). The extension of our measurements into the highly underdoped region of the

cuprate phase diagram, where κ/T becomes very small, led us to refine this extrapolation technique.

To motivate why this may be necessary, consider the possible scattering mechanisms available to a phonon impinging upon the surface of a crystal. The phonon may either be absorbed and reemitted with an energy distribution given by the local temperature (diffuse scattering) or it may be reflected elastically (specular reflection). In the case of diffuse scattering, the phonon is reradiated in a random direction resulting in a temperature independent value of Λ_0 and a T^3 dependence of κ_{ph} as recognized by Casimir.[41] However, as the temperature of a crystal is reduced and the average phonon wavelength increases, a surface of a given roughness appears smoother, which may increase the occurrence of specular reflection and result in a mean free path which varies as some power of temperature, so that $\kappa_{ph} \propto T^\alpha$. We would thus expect a deviation from the diffuse scattering limit of T^3 temperature dependence of κ_{ph} for samples with sufficiently smooth surfaces. Such an effect has been previously observed in many studies of low-temperature phonon heat transport in high quality crystals, such as Al_2O_3,[42] Si,[43] KCl and KBr,[44] LiF,[45] and diamond.[46]

This effect can be seen in most of our samples, manifesting itself as a gradual curvature in the low-temperature part of our data when plotted as κ/T vs T^2 (see Figs. 2 and 3). In light of this, the thermal conductivity in the boundary scattering regime is more correctly modeled as

$$\kappa = \kappa_{el} + \kappa_{ph} = AT + BT^\alpha \tag{A2}$$

with $\alpha < 3$. Here A is the coefficient of the electronic linear term, and B the temperature-independent coefficient of the phonon term, where α is some power of temperature, typically between 2 and 3. (Note that there is no fundamental reason for a single power law—it is simply an empirical result. For example, in Al_2O_3 previous studies[42] have found $\alpha = 2.77$.)

In superconductors possessing an isotropic or s-wave gap, the absence of an electronic linear term at low temperatures reveals this effect well. Plotted in Fig. 8 is thermal conductivity data for the s-wave superconductor V_3Si,[47] where the line is the result of a free fit to a simple power law as in Eq. (9). Such a procedure yields a linear term $A = -0.04 \pm 1$ μW K^{-2} cm^{-1}, a phonon coefficient $B = 5.73 \pm 0.07$ mW K$^{-(\alpha+1)}$ cm^{-1}, and an exponent $\alpha = 2.74 \pm 0.01$. The validity of such a fitting procedure is best seen by plotting the data as in Fig. 8, with the x axis in units of $T^{\alpha-1}$. The striking linearity of the data on this plot, and the fact that it extrapolates to zero, is good evidence for the appropriateness of the power law fitting procedure.

Figure 9 shows the results of a fit to Eq. (9) for our $YBCO_{6.6}$ crystal, where a power law of $\alpha = 2.71$ is seen to persist to temperatures as high as 550 mK. Power-law fits are also shown in Fig. 3(b), this time on a κ/T vs T^2 plot, for underdoped LSCO samples. The value of α observed in our samples was found to vary over a range from 2.4 for the YBCO $y = 6.99$ crystal to 2.92 for the LSCO $x = 0.09$ crystal.

It is worth stressing that the single-power-law fitting procedure described here is simply an empirical approach to
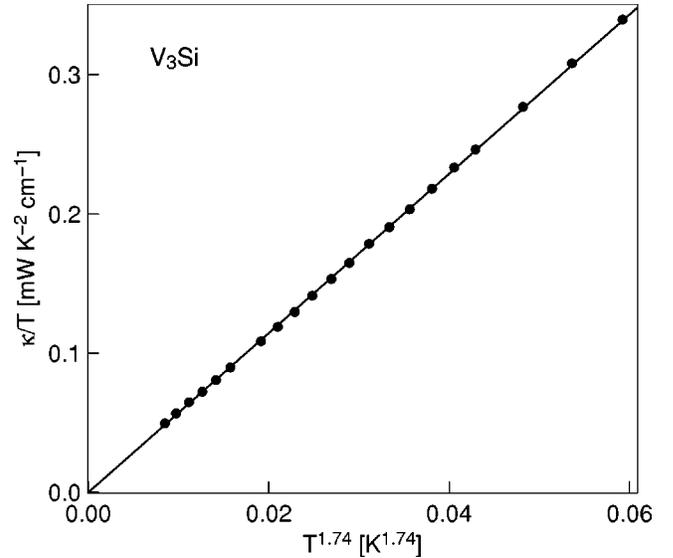
FIG. 8. Thermal conductivity of the s-wave superconductor V_3Si. The data are plotted as κ/T vs $T^{1.74}$, and the line represents a free fit to the data of the form of Eq. (A2). The resulting linear term is zero: 0 ± 1 μW K^{-2} cm^{-1}, consistent with that expected for a nodeless superconductor.

extrapolate the most reliable value of κ/T at $T = 0$. As a three-parameter *free* fit to the data over a temperature range typically of a decade (50–500 mK), it is far better than the old two-parameter *forced* fit to a $\kappa/T = a + bT^2$ form, which invariably must be limited to the very lowest temperatures (usually below 150 mK or so) and typically overestimates the value of κ_0/T. However, it must be noted that in some cases it does not work well over the whole range up to ~ 500 mK. This is indeed the case in our LSCO samples $x = 0.17$ and $x = 0.20$, where the single-power-law fit is inad-
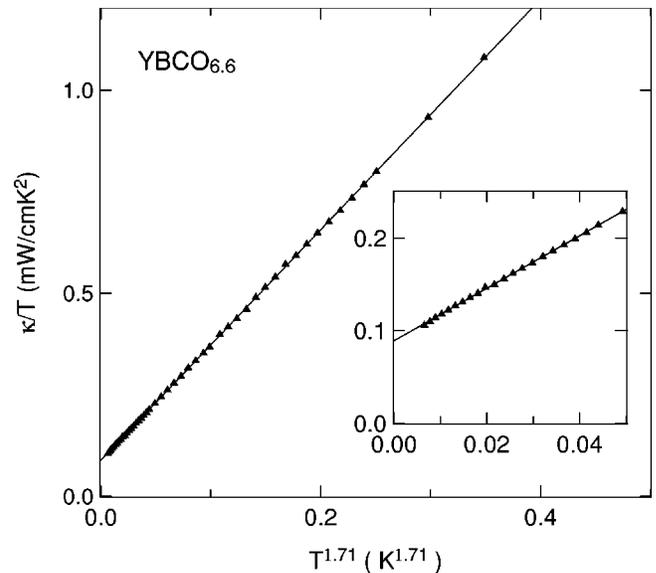
FIG. 9. Thermal conductivity of $YBCO_{6.6}$. The data are plotted as κ/T vs $T^{1.71}$, and the line is a linear fit. Inset: zoom at low temperatures. Note the presence of a clear residual linear term, the contribution of nodal quasiparticles.

equate to describe the rapid fall of κ/T below 150 mK. (Such a decrease was also observed in LSCO samples with similar doping levels in a previous study.[18]) The low-temperature drop is most likely in the electronic channel $[\kappa_e(T)]$, but its origin is as yet unclear. A downturn in κ/T at temperatures below 0.2 K or so can be induced in a sample on purpose by simply using highly resistive contacts (kΩ or higher). The drop is then attributed to the rapid deterioration of the coupling between electrons and phonons at those very low temperatures. In such a case, the extrapolation procedure must be based only on data above the downturn. It is not clear that the same phenomenon can still occur in the presence of excellent contacts, like those used here (less than 1 Ω). These considerations are explored and discussed more fully elsewhere.[48] In conclusion, when a single-power law works over a wide range of temperature (e.g., up to 0.5 K), then the extrapolation is reliable; if it does not work, then one needs to understand why and may be forced to rely only on data above any anomalous downturns. Note, however, that when it comes to extrapolating very small residual linear terms, as is done in Ref. 27 where the localized vs delocalized nature of the low-energy excitations is investigated, it becomes essential not only to use this more accurate procedure but also to go down to the very lowest temperatures.

In this paper, all data were successfully analyzed using the power-law procedure, except for LSCO samples $x=0.17$ and $x=0.20$, where instead a linear fit to the data in Fig. 3(a) was used below 150 mK, yielding the values of κ_0/T quoted in Table I. Use of a power-law fit above 150 mK yields higher values, namely $\kappa_0/T=0.2$ and 0.4 mW K^{-2} cm^{-1}, respectively, which has no impact on any of our conclusions.

---

*Present address: Laboratoire National des Champs Magnétiques Pulsés, 143 avenue de Rangueil, 31432 Toulouse, France.

†Present address: Department of Physics, Cornell University, Ithaca, NY 14853, USA.

‡Present address: Départment de physique, Université de Sherbrooke, Sherbrooke, Québec, Canada.

[1] P. Hirschfeld, P. Vollhardt, and P. Wölfle, Solid State Commun. **59**, 111 (1986).

[2] S. Schmitt-Rink, K. Miyake, and C. M. Varma, Phys. Rev. Lett. **57**, 2575 (1986).

[3] P. A. Lee, Phys. Rev. Lett. **71**, 1887 (1993).

[4] A. C. Durst and P. A. Lee, Phys. Rev. B **62**, 1270 (2000).

[5] L. Taillefer, B. Lussier, R. Gagnon, K. Behnia, and H. Aubin, Phys. Rev. Lett. **79**, 483 (1997).

[6] S. Nakamae, K. Behnia, L. Balicas, F. Rullier-Albenque, H. Berger, and T. Tamegai, Phys. Rev. B **63**, 184509 (2001).

[7] M. Chiao, R. W. Hill, C. Lupien, L. Taillefer, P. Lambert, R. Gagnon, and P. Fournier, Phys. Rev. B **62**, 3554 (2000).

[8] C. Proust, E. Boaknin, R. W. Hill, L. Taillefer, and A. P. Mackenzie, Phys. Rev. Lett. **89**, 147003 (2002).

[9] T. Timusk and B. Statt, Rep. Prog. Phys. **62**, 61 (1999).

[10] R. Liang, D. A. Bonn, and W. N. Hardy, Physica C **304**, 105 (1998).

[11] M. R. Presland, J. L. Tallon, R. G. Buckley, R. S. Liu, and N. E. Flower, Physica C **176**, 95 (1991).

[12] J. L. Tallon, C. Bernhard, H. Shaked, R. L. Hitterman, and J. D. Jorgensen, Phys. Rev. B **51**, 12 911 (1995).

[13] R. Liang, D. A. Bonn, and W. N. Hardy, Physica C **336**, 57 (2000).

[14] B. W. Veal, A. P. Paulikas, H. You, H. Shi, Y. Fang, and J. W. Downey, Phys. Rev. B **42**, 6305 (1990).

[15] W. N. Hardy, S. Kamal, D. A. Bonn, K. Zhang, R. Liang, E. Klein, D. C. Morgan, and D. Baar, Physica B **197**, 609 (1994).

[16] A. Hosseini, R. Harris, S. Kamal, P. Dosanjh, J. Preston, R. Liang, W. N. Hardy, and D. A. Bonn, Phys. Rev. B **60**, 1349 (1999).

[17] P. J. Hirschfeld and W. O. Putikka, Phys. Rev. Lett. **77**, 3909 (1996).

[18] J. Takeya, Y. Ando, S. Komiya, and X. F. Sun, Phys. Rev. Lett. **88**, 077001 (2002).

[19] M. J. Graf, S.-K. Yip, J. A. Sauls, and D. Rainer, Phys. Rev. B **53**, 15 147 (1996).

[20] J. Mesot, M. R. Norman, H. Ding, M. Randeria, J. C. Campuzano, A. Paramekanti, H. M. Fretwell, A. Kaminski, T. Takeuchi, T. Tokoya, *et al.*, Phys. Rev. Lett. **83**, 840 (1999).

[21] M. Vojta, Y. Zhang, and S. Sachdev, Phys. Rev. Lett. **85**, 4940 (2000).

[22] A. Sharoni, O. Millo, A. Kohen, Y. Dagan, R. Beck, G. Deutscher, and G. Koren, Phys. Rev. B **65**, 134526 (2002).

[23] R. W. Hill, C. Proust, L. Taillefer, P. Fournier, and R. L. Greene, Nature (London) **414**, 711 (2001).

[24] N. E. Hussey, S. Nakamae, K. Behnia, H. Takagi, C. Urano, S. Adachi, and S. Tajima, Phys. Rev. Lett. **85**, 4140 (2000).

[25] Y. Sun and K. Maki, Europhys. Lett. **32**, 355 (1995).

[26] G. S. Boebinger, Y. Ando, A. Passner, T. Kimura, M. Okuya, J. Shimoyama, K. Kishio, K. Tamasaku, N. Ichikawa, and S. Uchida, Phys. Rev. Lett. **77**, 5417 (1996).

[27] D. G. Hawthorn, R. W. Hill, C. Proust, F. Ronning, M. Sutherland, E. Boaknin, C. Lupien, M. A. Tanatar, J. Paglione, S. Wakimoto, H. Zhang, L. Taillefer, T. Kimura, M. Nohara, H. Takagi, and N. E. Hussey, cond-mat/0301107, Phys. Rev. Lett. (to be published).

[28] W. A. Atkinson and P. J. Hirschfeld, Phys. Rev. Lett. **88**, 187003 (2002).

[29] J. C. Campuzano, H. Ding, M. R. Norman, H. M. Fretwell, M. Randeria, A. Kaminski, J. Mesot, T. Takeuchi, T. Sato, T. Yokoya, T. Takahashi, T. Mochiku, K. Kadowaki, P. Guptasarma, D. G. Hinks, Z. Konstantinovic, Z. Z. Li, and H. Raffy, Phys. Rev. Lett. **83**, 3709 (1999).

[30] M. R. Norman, H. Ding, M. Randeria, J. C. Campuzano, T. Yokoya, T. Takeuchi, T. Takahashi, T. Mochika, K. Kadowaki, P. Guptasarma, and D. G. Hinks, Nature (London) **392**, 157 (1998).

[31] P. J. White, Z.-X. Shen, C. Kim, J. M. Harris, A. G. Loeser, P. Fournier, and A. Kapitulnik, Phys. Rev. B **54**, R15 669 (1996).

[32] A. G. Loeser, Z.-X. Shen, M. C. Schabel, C. Kim, M. Zhang, A. Kapitulnik, and P. Fournier, Phys. Rev. B **56**, 14 185 (1996).

[33] Z.-X. Shen (private communication).

[34] C. Panagopoulos and T. Xiang, Phys. Rev. Lett. **81**, 2336 (1998).

[35] H. Ding, M. R. Norman, J. C. Campuzano, M. Randeria, A. F. Bellman, T. Yokoya, T. Takahashi, T. Mochiku, and K. Kad-

owaki, Phys. Rev. B **54**, R9678 (1999).

[36] E. Fradkin, Phys. Rev. B **33**, 3263 (1986).

[37] S. Chakravarty, R. B. Laughlin, D. K. Morr, and C. Nayak, Phys. Rev. B **63**, 094503 (2001).

[38] X. Yang and C. Nayak, Phys. Rev. B **65**, 064523 (2002).

[39] P. J. Turner, R. Harris, S. Kamal, M. E. Hayden, D. M. Broun, D. C. Morgan, A. Hosseini, P. Dosanjh, G. Mullins, J. S. Preston, R. Liang, D. A. Bonn, and W. N. Hardy, cond-mat/0111353 (unpublished).

[40] L. B. Ioffe and A. J. Millis, cond-mat/0112509; J. Phys. Chem. Solids (to be published).

[41] H. B. G. Casimir, Physica (Amsterdam) **5**, 495 (1938).

[42] R. O. Pohl and B. Stritzker, Phys. Rev. B **25**, 3608 (1982).

[43] W. S. Hurst and D. R. Frankl, Phys. Rev. **186**, 801 (1969).

[44] W. D. Seward, Ph.D. thesis, Cornell University, 1965.

[45] P. D. Thatcher, Phys. Rev. **156**, 975 (1967).

[46] R. Berman, F. E. Simon, and J. M. Ziman, Proc. R. Soc. London, Ser. A **220**, 171 (1953).

[47] E. Boaknin, M. A. Tanatar, J. Paglione, D. Hawthorn, F. Ronning, R. W. Hill, M. Sutherland, L. Taillefer, J. Sonier, S. M. Hayden, and J. W. Brill, Phys. Rev. Lett. **90**, 117003 (2003).

[48] J. Paglione, R. Hill, E. Boaknin, D. Hawthorn, M. Sutherland, L. Taillefer, R. Bel, and K. Behnia (unpublished).